

## Steady States and Dynamic Behavior of an LDPE Autoclave Reactor

Jinsuk Lee, °Kil Sang Chang\*, Jae-Yeon Kim\*, and Hyun-Ku Rhee

Dep. of Chem. Eng., Seoul National University  
\* Hanyang Chemical Corporation Research Center

A two compartmented autoclave reactor for the polymerization of low density polyethylene is analyzed with respect to the effects of heat transfer and operation variables. Each compartment being considered as a completely mixed cell, two CSTRs model is proposed. The system shows various multiplicity features of steady state and periodic oscillatory motions. Heat removal efficiency and initiator supplement appear to have significant effect on the conversion of monomer with the temperature properly maintained, which should be taken into account in the reactor design.

## INTRODUCTION

Polyethylene is one of the most useful thermoplastic resins, and the worldwide production is incessantly increasing for its large industrial applications. Polyethylenes of high molecular weight are generally produced in two density grades depending on the reacting conditions. The low density materials(LDPE) of roughly 50 % crystallinity requires polymerization of ethylene at 1000 to 2500 atm and temperatures of 100-300 °C in the presence of a peroxide catalyst. Commercially vessel and tubular reactors are generally in use.

A vessel reactor, termed as an autoclave, is designed with a high aspect ratio, divided into two or more compartments in series by fixed or rotating discs. Also, characterized by high heat generation, high viscosity and poor heat transfer, the reactor, stirred by an impeller mounted on unique shaft, requires a high power input to maintain good mixing conditions in each compartment. The reaction progresses rapidly and large amount of heat is generated. However, due to the enormous wall thickness of the reactor, heat removal efficiency is very low, and the temperature is controlled through a control system that acts on the initiator injection pump. Therefore, the performance with respect to the productivity or conversion rate, excluding the product quality, is directly connected with the initiator consumption rate. Since vessel reactors are designed for broad operating conditions, very highly skilled techniques are required to obtain various qualities of product meeting market demand.

Due to the particular reaction conditions of the LDPE processes, there have not been reported sufficient kinetic and operational data. Even the kinetic data reported by several authors[1-9] are not consistent with one another. So that many problems still arise in the reactor operation as well as in the analysis. Here to investigate the steady states and dynamic responses of a two compartmented autoclave reactor, we propose two CSTRs model considering each compartment as a completely mixed cell with cooling jacket. The feed materials are introduced into each cell with fixed temperature and concentration. Since the changes in operation parameters can directly affect the state of the reactor and the output of the first cell acts as a forcing to the second, the steady state and dynamic

response becomes very complicated and remains far from our prediction.

Focused on a CSTR or CSTRs in series, some models for free radical polymerization system have been studied by several authors[2,3,5,10-12] concerning the stability analysis and control problems. Finite number of discrete cell model may not exactly interpret the degree of mixing and thermal gradients of the reactor, because industrial reactors are usually known far from completely mixed. However, such studies can provide us with valuable insight into the process almost precisely, although more facts are still to be explored. Our study intends to examine, through the variations of monomer conversion and reactor temperatures, how the reactor states are affected by the heat transfer and the operation parameters.

## THE REACTOR MODEL

LDPE polymerization reaction proceeds by a free radical mechanism which takes place in a homogeneous phase. A very general reaction steps to be considered are the initiation, propagation and termination. The physical properties of the reacting medium, which may vary depending on the conversion and temperature, are assumed to be constant throughout the analysis. The reaction rate constants are also assumed independent of the polymer chain lengths. Then for two CSTRs as shown schematically in Fig. 1, the mass balances of monomer, initiator, and living polymers and energy balance lead to a set of eight ordinary differential equations, and can be expressed in dimensionless form as follows.

For the cell 1:

$$\begin{aligned} \mu dx_1/d\tau = & -\alpha x_1 - \mu [2\phi f y_1 D_{a1} \exp(\gamma_d - \gamma_d/w_1) \\ & + x_1 z_1 D_{aP} \exp(\gamma_P - \gamma_P/w_1)] \end{aligned} \quad (1)$$

$$\mu dy_1/d\tau = \alpha - \alpha y_1 - \mu y_1 D_{a1} \exp(\gamma_d - \gamma_d/w_1) \quad (2)$$

$$\begin{aligned} \mu dz_1/d\tau = & -\alpha z_1 + \mu [2\phi f y_1 D_{a1} \exp(\gamma_d - \gamma_d/w_1) \\ & - z_1^2 D_{a1} \exp(\gamma_t - \gamma_t/w_1)] \end{aligned} \quad (3)$$

$$\mu dw_1/d\tau = \alpha - \alpha w_1 + \mu [x_1 z_1 B_P D_{aP} \exp(\gamma_P - \gamma_P/w_1)]$$

$$+z_1^2 B_t D_a \exp(\gamma_t - \gamma_t/w_1) - \delta(w_1 - w_c)] \quad (4)$$

For the cell 2:

$$(1-\mu) dx_2/d\tau = 1 - \alpha + \alpha x_1 - x_2 - (1-\mu) [2\phi f y_2 D_a \exp(\gamma_d - \gamma_d/w_2) + x_2 z_2 D_a \exp(\gamma_p - \gamma_p/w_2)] \quad (5)$$

$$(1-\mu) dy_2/d\tau = 1 - \alpha + \alpha y_1 - y_2 - (1-\mu) y_2 D_a \exp(\gamma_d - \gamma_d/w_2) \quad (6)$$

$$(1-\mu) dz_2/d\tau = \alpha z_1 - z_2 + (1-\mu) [2\phi f y_2 D_a \exp(\gamma_d - \gamma_d/w_2) - z_2^2 D_a \exp(\gamma_t - \gamma_t/w_2)] \quad (7)$$

$$(1-\mu) dw_2/d\tau = 1 - \alpha + \alpha w_1 - w_2 + (1-\mu) [x_2 z_2 B_p D_a \exp(\gamma_p - \gamma_p/w_2) + z_2^2 B_t D_a \exp(\gamma_t - \gamma_t/w_2) - \delta(w_2 - w_c)] \quad (8)$$

Here the heat effects by the initiation reaction and the chain transfer effects are neglected. The dimensionless parameters used in the equations are defined as:

$$x_i = M_i/M_f, \quad y_i = I_i/I_f, \quad z_i = G_i/M_f, \quad w_i = T_i/T_f, \quad \text{for } i=1,2$$

$$\tau = tq_0/V, \quad \delta = UA/\rho q_0 C_p, \quad \phi = I_f/M_f, \quad \mu = V_1/V, \quad w_c = T_c/T_f$$

$$\alpha = q_1/q_0, \quad \gamma_d = E_d/RT_f, \quad \gamma_p = E_p/RT_f, \quad \gamma_t = E_t/RT_f$$

$$B_p = (-\Delta H_p)M_f/\rho C_p T_f, \quad B_t = (-\Delta H_t)M_f/\rho C_p T_f$$

$$D_a = V k_{d0} \exp(-\gamma_d)/q_0, \quad D_a p = V M_f k_{p0} \exp(-\gamma_p)/q_0$$

$$D_a t = V M_f k_{t0} \exp(-\gamma_t)/q_0$$

The steady states can be obtained by solving eight nonlinear algebraic equations letting all the derivative terms equal to zero. However, the highly nonlinear property of the system brings about the multiplicity problem of solution, which makes the global analysis very difficult. When there exist multiple steady states, the stable steady states share the attraction regions in the phase space and may produce quite different grades of product. To solve the steady state behavior of a system, it is often convenient to examine the dependence of a solution on a

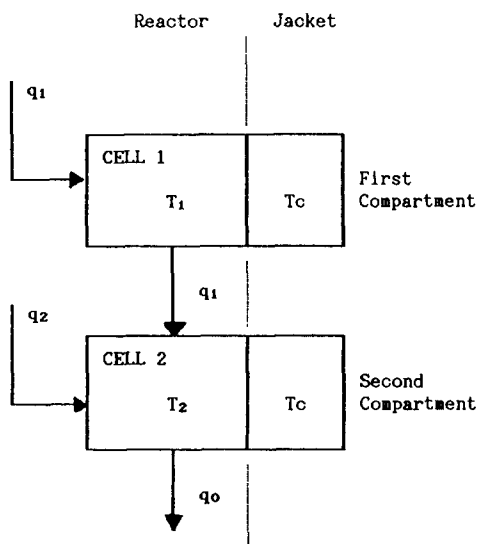


Fig. 1. Schematic diagram of two compartmented autoclave reactor model.

distinguished parameter. Bifurcation theory[13-15] will be of great help for the comprehensive analysis of a nonlinear parameter system.

A large class of bifurcation problems with nonlinear parameter systems can be solved numerically. The complete numerical method has been analyzed by H.B. Keller[16], implemented by the techniques of continuation of general solution branch with implicit function theorem and of branch switching at singular points, and a practically useful software was written by E. J. Doedel, called AUTO[17]. The original method can be applied to the general N-dimensional steady state equations, and therefore the above eight equations can be used directly to the program AUTO, which can provide us with regular and periodic solution branches of the system with the informations on the stability properties. The program can also compute the locus of steady state limit points dividing the multiplicity regions on parameters plane, and the locus of Hopf bifurcation points[18,19] from which emerges a periodic oscillatory motion.

## RESULTS AND DISCUSSION

Heat removal effect in the autoclave reactor, which has been usually neglected in the reactor analysis for its enormous wall thickness, may have a great influence with the initiator feed rate on the conversion efficiency and control policy. Taking the heat transfer coefficient  $\delta$  and the initiator feed rate  $\phi$  as changing parameters, with the other parameters fixed as shown in Table 1, steady state and dynamic features are investigated in some detail. The calculation result suggests various and interesting multiplicity features of steady state and dynamic character of limit cycles for feasible parameter regions.

Fig. 2 illustrates on the  $(\delta, \phi)$ -plane the multiplicity regions of steady states and the loci of Hopf bifurcation points. Here, we notice that the number of steady states increases or decreases by the number of two when a solid line is crossed over, and that for large area of low  $\delta$  and high  $\phi$  the reactor state can be complex having up to five steady states. The locus of Hopf points shown by a dashed line divides the plane into regions of different dynamic stabilities. The dynamic characters may appear quite differently depending on the regions divided by solid or dashed lines.

Now fixing  $\delta = 2.34$  and taking  $\phi$  as a parameter, the bifurcation diagram is shown in Fig. 3. For an operation parameter range, two hysteresis features of steady state and periodic oscillatory motions are found as can be expected from Fig. 2. Two periodic solution

Table 1. The values of dimensionless parameters used in the model analysis.

Dimensionless parameter	Numerical value
$B_p$	4.3329
$B_t$	1.9859
$D_a d$	$1.3854 \times 10^{-5}$
$D_a p$	$4.6175 \times 10^4$
$D_a t$	$1.2163 \times 10^8$
$f$	1
$w_c$	4/3
$\alpha$	0.5
$\gamma_d$	$4.2456 \times 10^4$
$\gamma_p$	8.7989
$\gamma_t$	6.6264
$\mu$	5/12

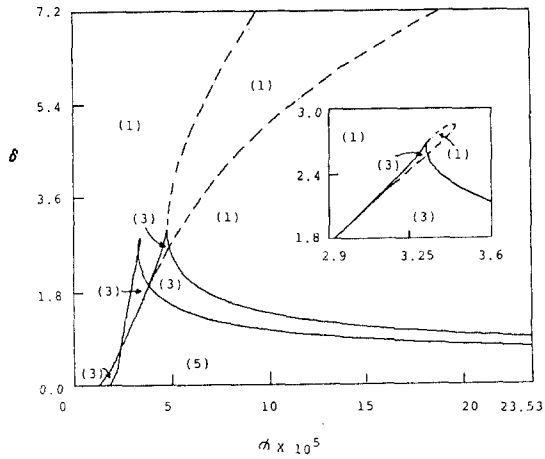


Fig. 2. Multiplicity regions of steady state and Hopf bifurcation points.

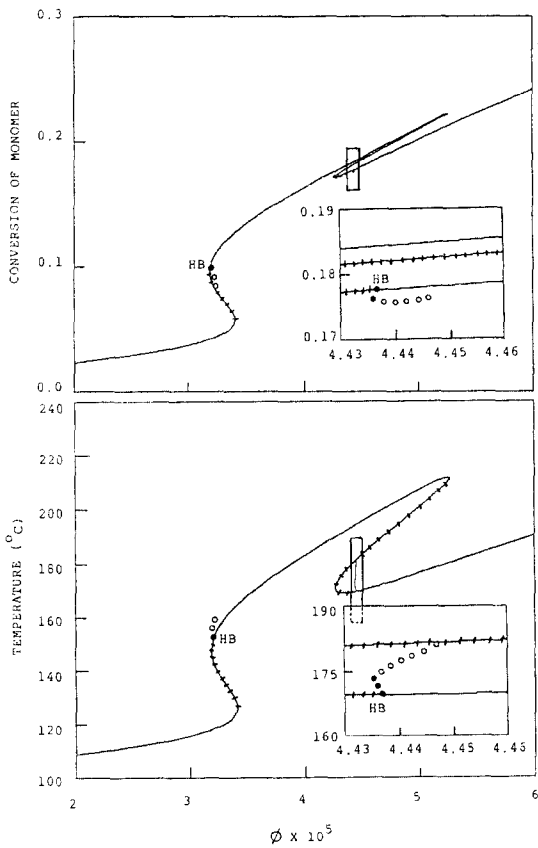


Fig. 3. Parametric change of steady states and Hopf bifurcation points when  $\delta = 2.34$ .

branches emanating from independent Hopf points die away coalescing with the homoclinic orbit of an unstable saddle point. One notable thing is that a stable periodic branch, created by a supercritical Hopf bifurcation, loses its stability at the turning point, called tangent bifurcation, and an unstable periodic branch prevails until it dies away. One may note that an unstable limit cycle acts as a boundary of neighboring attractors like an unstable saddle point. Typical stable and unstable limit cycles are drawn in Fig. 4 with their dynamic patterns. The trajectories emanating from the unstable steady state or from the unstable limit cycle tend to the stable limit cycle. The number of steady states and their dynamic patterns, depending on the parametric range of  $\delta$ , are tabulated in Table 2.

When the heat transfer coefficient increases, to  $\delta = 2.7$  in Fig. 2, we expect one hysteresis feature of steady state and three Hopf bifurcation points. Fig. 5 illustrates the bifurcational features of steady states and periodic motions, in which two Hopf points are paired and linked by a stable periodic branch and, we note, another periodic branch from other Hopf point undergoes a couple of tangent bifurcations and a homoclinic explosion. Parametric data are given in Table 3. Transient behaviors of conversion and temperature of a periodic oscillation are shown in Fig. 6. One may note here that the mean conversion of the

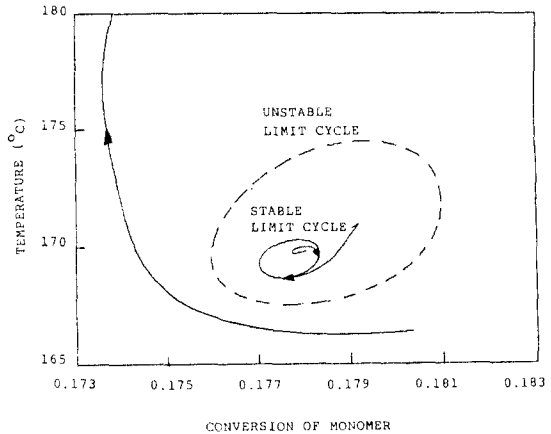


Fig. 4. Phase trajectories of stable and unstable limit cycles when  $\delta = 2.34$  and  $\phi = 4.436471 \times 10^{-5}$ .

Table 2. Number of steady states and dynamic patterns in various ranges of  $\phi$  with  $\delta = 2.34$ .

$\phi \times 10^5$	stable focus or node	unstable focus or saddle point	stable limit cycle	unstable limit cycle
0-3.187125	1			
-3.202375	1	2		
-3.206862	2	1		1
-3.406331	2	1		
-4.262534	1			
-4.435402	1	2		
-4.436947	1	2	1	1
-4.447409	2	1		1
-5.269688	2	1		
$-\infty$	1			

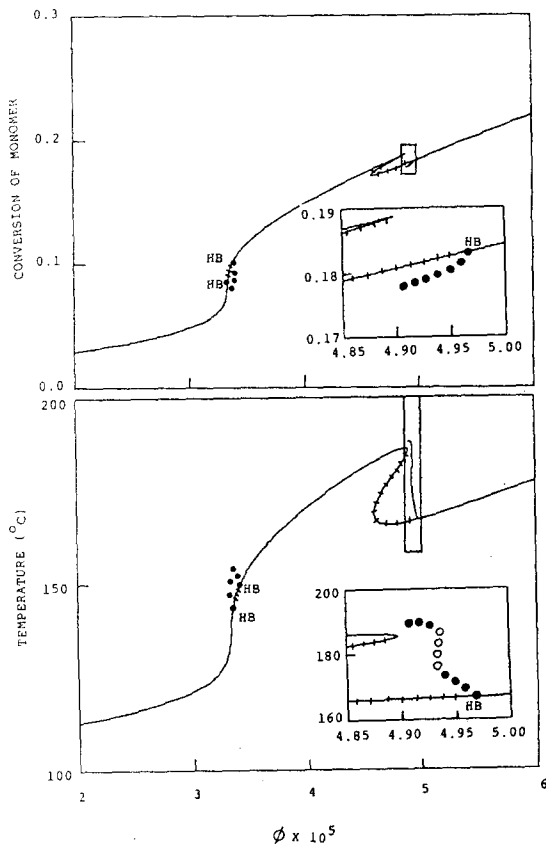


Fig. 5. Parametric change of steady states and Hopf bifurcation points when  $\delta=2.7$ .

Table 3. Number of steady states and dynamic patterns in various ranges of  $\phi$  with  $\delta=2.7$ .

$\phi \times 10^5$	stable focus or node	unstable focus or saddle point	stable limit cycle	unstable limit cycle
0-3.334297	1			
-3.339713		1	1	
-4.594764	1			
-4.897554	1	2		
-4.931898		1	1	
-4.934634		1	1	2
-4.970440		1	1	
$-\infty$	1			

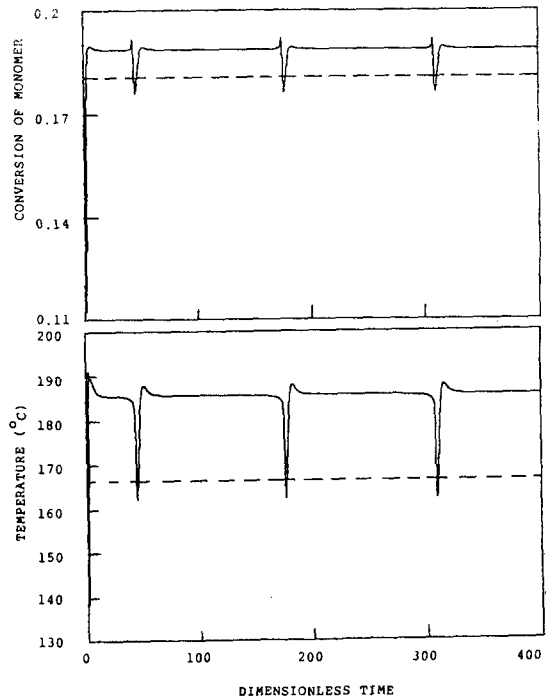


Fig. 6. Transient behaviors of conversion rate and temperature of a periodic oscillation when  $\delta=2.7$  and  $\phi=4.897588 \times 10^{-5}$ .

oscillation seems obviously much higher than the value of unstable steady state. This means that if the operation parameters are set in this region the periodic operation is more effective than the steady state operation though this can be stabilized with the help of control system. This phenomenon does not occur very often in usual reactor operation. However, this fact shows that it can be sometimes beneficial to adopt a periodic operation.

Another case of  $\delta=3.6$  has been studied with a bifurcation diagram as shown in Fig. 7. Here we have a unique steady state over the whole range of parameter and two Hopf points linked by a periodic branch which has one turning point. Taking  $\phi=4.982353 \times 10^{-5}$ , a limit cycle is drawn in Fig. 8, which shows seemingly doubly periodic on an invariant torus. This behavior can be found when a periodic branch loses its stability by a modulus of a complex Floquet multiplier crossing over the unit circle. Thorough investigation of this bifurcational feature is beyond the scope of the present study and left for later work. Meanwhile, as can be seen from these bifurcation diagrams, heat transfer directly effects the temperature reduction of reacting medium at a fixed initiator concentration. However, under the temperature allowance of the reactor, the gross rates of initiation and propagation can be enhanced further by increasing the initiator concentration, and this will consequently increase the conversion of the monomer.

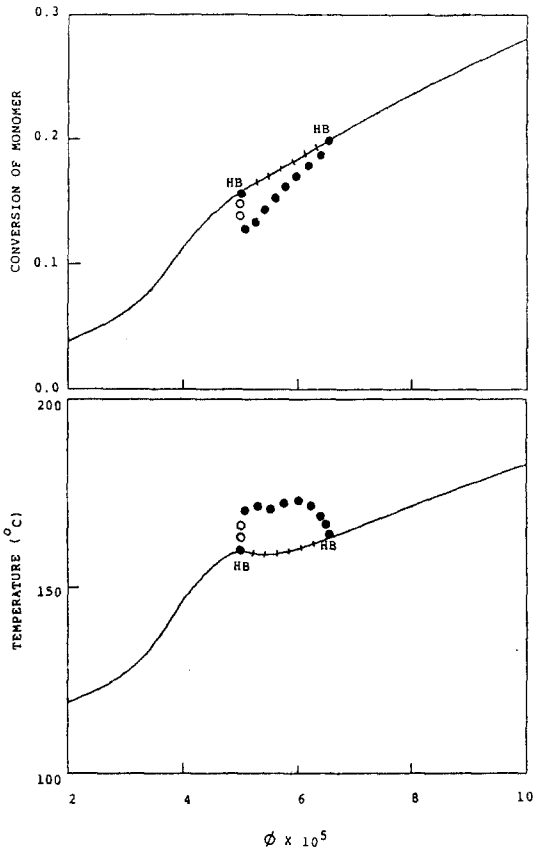


Fig. 7. Parametric change of steady states and Hopf bifurcation points when  $\delta=3.6$ .

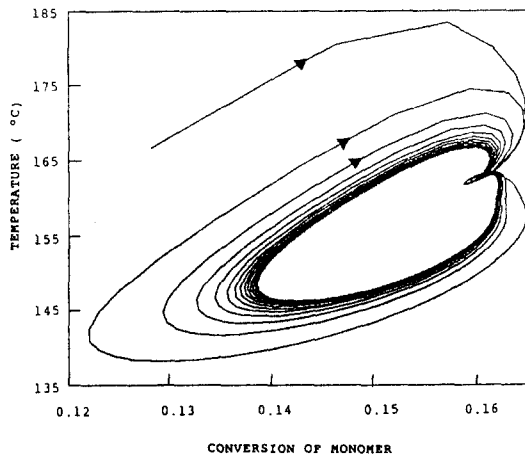


Fig. 8. Phase trajectory of a limit cycle showing seemingly doubly periodic on an invariant torus when  $\delta=2.34$  and  $\phi=4.436471 \times 10^{-5}$ .

## CONCLUSION

With these model predictions we understand that the LDPE reaction in an autoclave exhibits very complex behaviors of steady state and dynamics. The multiplicity features are occasionally very sensitive to some parameter changes, and the stable steady states and limit cycles possess their own attraction regions in the phase space. Since any perturbation in steady state operation is not allowed beyond its attraction region, a rigorous control policy should be adopted concerning the start-up and steady state operation. Furthermore, effective heat removal and initiator supplement can enhance the monomer conversion significantly without the temperature lift-up jeopardizing the safety aspect of the reactor. The reactor design should be developed in this respect for the maximum performance.

## NOTATION

- A : area( $m^2$ )
- B : dimensionless heat of reaction
- $C_p$  : heat capacity(cal/g · K)
- Da : Damköhler number
- E : activation energy(cal/gmol)
- f : initiator efficiency factor
- G : concentration of living polymer(mol/l)
- $-\Delta H$  : heat of reaction(cal/gmol)
- I : concentration of initiator(mol/l)
- k : Arrhenius preexponential facto( $sec^{-1}$ for decomposition; l/mol-sec for propagation and termination reactions)
- M : concentration of monomer(mol/l)
- q : flow rate(l/sec)
- t : time(sec)
- T : temperature(K)
- U : heat transfer coefficient(cal/g ·  $m^2$  · sec)
- V : reactor volume(l)
- w : dimensionless temperature
- x : dimensionless concentration of monomer
- y : dimensionless concentration of initiator
- z : dimensionless concentration of living polymer

## Greek letters

- $\alpha$  : feed flow rate ratio
- $\gamma$  : dimensionless activation energy
- $\delta$  : dimensionless heat transfer coefficient
- $\mu$  : cell volume ratio
- $\rho$  : density of reacting medium(g/l)
- $\tau$  : dimensionless time
- $\phi$  : ratio of initiator feed concentration to monomer feed concentration

## Subscripts

- 1,2 : reactor cell number
- c : coolant
- d : decomposition
- f : feed
- p : propagation
- t : termination

## REFERENCES

1. C. H. Chen, J. G. Vermeychuk, J. A. Howell and P. Ehrlich, "Computer model for tubular high pressure polyethylene reactors," AICHE. J., vol.22, 463(1976).
2. G. Donati, M. Gramondo, E. Langianni and L. Marini, "Low density polyethylene in vessel reactors," Ing. Chim. Ital., vol.17, 88(1981).
3. L. Marini and C. Georgakis, " Low-density polyethylene vessel reactors," AICHE. J., vol.30, 401(1984).
4. S. Agrawal and C. D. Han, "Analysis of the high pressure polyethylene tubular reactor with axial mixing," AICHE. J., vol.21, 449(1975).
5. J. S. Shastry and L. T. Fan, "Stability analysis in polymerization reactor systems," Chem. Eng. J., vol.6, 129(1973).
6. G. Luft and H. Seidel, "Metering of peroxide polymerization initiators at elevated pressure," Die Angewandt Macromol., vol.86, 93(1980).
7. S. Goto, K. Yamamoto, S. Furui and M. Sugimoto, J. ppl. Polym. Sci., vol.36, 21(1981).
8. W. Hollar and P. Ehrlich, "An improved model for temperature and conversion profiles in tubular high pressure polyethylene reactors," ACS Symp. Ser., March(1983).
9. A. Brandolin, N. J. Capiati, J. N. Farber and E. M. Valles, "Mathematical model for high-pressure tubular reactor for ethylene polymerization," Ind. Eng. Chem., vol.27, 784(1988).
10. L. S. Henderson, "Stability analysis of polymerization in continuous stirred-tank reactors," Chem. Eng. Prog., March, 42(1987).
11. B. W. Brooks, "Dynamic behavior of a continuous-flow polymerization reactor," Chem. Eng. Sci., vol.36, 589(1981).
12. K. Y. Choi, "Analysis of steady state of free radical solution polymerization in a continuous stirred tank reactor," Pol. Eng. Sci., vol.26, 975(1986).
13. T. Brocker and L. Lander, "Differential germs and catastrophes," Cambridge University Press, 1975.
14. Y. C. Lu, "Singularity theory and an introduction to catastrophe theory," Springer-Verlag, New York, 1976.
15. R. G. Gilmore, "Catastrophe theory for scientists and engineers," Wiley, New York, 1981.
16. H. B. Keller, "Numerical solution of bifurcation and nonlinear eigenvalue problems," in Applications of Bifurcation Theory, P.H. Rabinowitz ed., Academic Press, 1977.
17. E. J. Doedel, "AUTO: A program for the automatic bifurcation analysis of autonomous systems," Cong. Num., vol. 30, 265(1981).
18. J.E. Marsden and M. McCracken, "The Hopf bifurcation and its applications," Springer-Verlag, New York, 1976.
19. G. Iooss and D. D. Joseph, "Elementary stability and bifurcation theory," Springer-Verlag, New York, 1980.